ELSEVIER

Contents lists available at ScienceDirect

Chemistry and Physics of Lipids

journal homepage: www.elsevier.com/locate/chemphyslip





Thermal stability of bivalent cation/phosphoinositide domains in model membranes

Trevor A. Paratore, Greta E. Schmidt, Alonzo H. Ross, Arne Gericke

Worcester Polytechnic Institute, Department of Chemistry and Biochemistry, Worcester, MA 01609, USA

ARTICLE INFO

Keywords: Phosphoinositide PIP2 PIP3 PI(4)P PI(4,5)P2 PI(3,4,5)P3

ABSTRACT

As key mediators in a wide array of signaling events, phosphoinositides (PIPs) orchestrate the recruitment of proteins to specific cellular locations at precise moments. This intricate spatiotemporal regulation of protein activity often necessitates the localized enrichment of the corresponding PIP. We investigate the extent and thermal stabilities of phosphatidylinositol-4-phosphate (PI(4)P), phosphatidylinositol-4,5-bisphosphate (PI(4,5) P_2 and phosphatidylinositol-3,4,5-trisphosphate (PI(3,4,5) P_3) clusters with calcium and magnesium ions. We observe negligible or minimal clustering of all examined PIPs in the presence of M_2^{2+} ions. While PI(4)P shows in the presence of M_2^{2+} no clustering, PI(4,5) M_2^{2+} forms with M_2^{2+} strong clusters that exhibit stablity up to at least M_2^{2+} or M_2^{2+} is less than what was observed for PI(4,5) M_2^{2+} , yet we still observe some clustering up to M_2^{2+} or M_2^{2+} is less than what was observed for PIP clustering, we examined whether bivalent cations and cholesterol has been demonstrated to enhance PIP clustering, we examined whether bivalent cations and cholesterol synergistically promote PIP clustering. We found that the interaction of M_2^{2+} or M_2^{2+} with PI(4)P remains extraordinarily weak, even in the presence of cholesterol. In contrast, we observe synergistic interaction of cholesterol and M_2^{2+} with PI(4,5) M_2^{2+} remains weak. PI(3,4,5) M_2^{2+} does not show strong clustering with cholesterol for the experimental conditions of our study and the interaction with M_2^{2+} and M_2^{2+} was not influenced by the presence of cholesterol.

1. Introduction

Phosphoinositides (PIPs) are a family of phospholipids obtained through phosphorylation of phosphatidylinositol (PI) at the 3, 4 and 5 positions of the inositol ring headgroup. The interconversion of the seven PIPs is facilitated by kinases and phosphatases specific for distinct phosphoinositides, resulting in tight regulation in space and time (Viaud al.. 2016). Within the plasma membrane phosphatidylinositol-4-phosphate (PI(4)P),phosphatidylinositol-4. 5-bisphosphate $(PI(4,5)P_2)$ and phosphatidylinositol-3,4, 5-trisphosphate regulate processes such as cytoskeletal rearrangement, vesicular trafficking, membrane fusion, cell proliferation, and cell growth (Bura et al., 2023; Katan and Cockcroft, 2020; Mandal, 2020; Siess and Leonard, 2019). Many of these processes are associated with localized accumulation of PIPs (Cabral-Dias and Antonescu, 2022; Conduit et al., 2021; Fratini et al., 2021; Katan and Cockcroft, 2020; Li et al., 2022; Li et al., 2020; Myeong et al., 2021; Redpath et al., 2020). In addition, the quantity of proteins binding to PIP species generally surpasses the cellular concentrations of the respective lipid (Catimel et al., 2008; Catimel et al., 2009; Overduin and Kervin, 2021; Palmieri et al., 2010). This relative paucity of PIPs in cellular membranes makes the interaction of proteins with PIPs highly contextual, i.e., PIPs need to accumulate in domain patches that have other cues for the respective protein to bind (e.g., binding to a second lipid that co-accumulates with the respective PIP in a domain). In compositionally diverse biological membranes, many factors contribute to the formation of lipid/protein enriched domains. The details of the processes that govern the assembly of these "platforms" are only just beginning to emerge.

At physiological pH, PI(4)P, PI(4,5)P₂ and PI(3,4,5)P₃ exhibit headgroup charges of about -2 (Owusu Kwarteng et al., 2021) -4 and -5 (Kooijman et al., 2009), respectively. It was therefore expected that mutual PIP interactions would display dominant repulsive forces. However, intramolecular hydrogen bond formation between the phosphomonoester and hydroxyl groups results in a smearing of the charge

Abbreviations: PI4P, Phosphatidylinositol-4-phosphate; PI4, 5P₂, Phosphatidylinositol-4,5-bisphosphate; PI3, 4,5P₃, Phosphatidylinositol-3,4,5-trisphosphate; POPC, Palmitoyloeloylphosphatidylcholine; DOPC, Dioeloylphosphatidylcholine; LUV, large unilamellar vesicle; MLV, multilamellar vesicle.

E-mail address: agericke@wpi.edu (A. Gericke).

^{*} Corresponding author.

around the ring and hence, a reduction of the charge density, while intermolecular hydrogen bond formation further distributes the charge along the interface (Kooijman et al., 2009; Levental et al., 2008; Slochower et al., 2013; Wang et al., 2014). This intricate balance between repulsive and attractive forces governs the extent of clustering in the absence of stronger PIP cluster-promoting species. Under these conditions, PIP clusters are extraordinarily fragile and the extent of clustering (if it even occurs) is strongly dependent on the effects of monovalent cations in the buffer. While in the presence of Na⁺ weak PIP clustering can be observed (Redfern and Gericke, 2004, 2005), it is virtually absent in the presence of K+. The PIP phosphomonoester groups are kosmotropic, while the phosphodiester group is chaotropic (for a review on the Hofmeister series see (Gregory et al., 2022; He and Ewing, 2023). The mildly kosmotropic Na⁺ interacts predominantly with the PIP phosphomonoester group (and only to a limited extent with the phosphodiester group), which leads to moderate PIP clustering (Han et al., 2020). In contrast, the chaotropic K⁺ interacts exclusively with the chaotropic phosphodiester group and virtually no clustering is observed (Han et al., 2020).

Cholesterol has been found to promote phosphoinositide clustering in model systems as well as in cells (Bucki et al., 2019; Graber et al., 2014; Jiang et al., 2014; Levental et al., 2009a; Levental et al., 2009b; Lolicato et al., 2022; Myeong et al., 2021; Wen et al., 2018). In lipid rafts (sphingolipid/cholesterol enriched domains), cholesterol interacts primarily with the lipid chains, which leads to an increased conformational order and for distinct cholesterol mole fractions this results in the formation of liquid-ordered phases. In the case of phosphoinositides, it is believed that the cholesterol hydroxyl group interacts with the PIP headgroup either directly or in a water mediated fashion (Jiang et al., 2014). This interaction leads to a stabilization of enriched phosphoinositide domains and while it is not possible to obtain phosphoinositide only vesicles, it is possible to fabricate phosphoinositide/cholesterol vesicles as long as the cholesterol mole fraction exceeds 20 % (Jiang et al., 2014).

Multivalent cations and cationic peptides and protein motifs have by far the strongest clustering effect on phosphoinositides. Physiological concentrations of Ca^{2+} and Mg^{2+} have been shown to cluster PI(4,5)P₂ (Wen et al., 2018, 2021). The clustering effect of these bivalent cations and cholesterol have been found to be synergistic (Jiang et al., 2014). Equally, cationic peptides or cationic amino acid clusters in proteins have been shown to cluster PIPs (Bucki et al., 2019; Drucker et al., 2013; Epand et al., 2004; Gambhir et al., 2004; Musse et al., 2008; Sarmento et al., 2021; Tong et al., 2008; Wang et al., 2002; Yoshioka et al., 2020).

The interaction of cations with phosphoinositides can be best understood by examining the Hofmeister series. K⁺ is chaotropic, Na⁺ is mildly kosmotropic, Ca2+ is kosmotropic and Mg2+ has the strongest kosmotropic characteristics among these cations. Phosphoinositides exhibit a chaotropic phosphodiester group (charge -1), a mildly kosmotropic single deprotonated phosphomonoester group (charge -1), while the double deprotonated phosphomonoester group is kosmotropic (Han et al., 2020). The "Law of Matching Water Affinities (LMWA)" (Collins, 1997) establishes that the tendency of a cation and anion to form a contact pair is governed by how closely their hydration energies match. In line with the LMWA, atom molecular dynamics (MD) simulations showed that the kosmotropic K⁺ interacts preferentially with the kosmotropic PIP phosphodiester group while having no clustering effect on PI(4,5)P₂ (Bradley et al., 2020; Han et al., 2020). Similarly, the mildly kosmotropic Na⁺ interacts with the phosphodiester and phosphomonoester groups promoting mild and fragile clustering, consistent with experimental findings (Redfern and Gericke, 2004, 2005). The MD studies further showed that Ca²⁺ ions rearrange their hydration shell to preferentially interact with the PIP phosphomonoester groups (and not with the phosphodiester group) leading to bridging (clustering) of two or three PIP molecules. However, Mg²⁺ ions bind tightly their hydration shell, preventing rearrangement, resulting in weak interaction with the PIP phosphomonoester group via its outer hydration shell (Bradley et al.,

2020; Han et al., 2020; Han et al., 2022). Consequently, Mg²⁺ has a limited PIP clustering effect.

While significant progress has been made to understand the physicochemical underpinnings of phosphoinositide clustering, there are still several pivotal questions awaiting resolution. Foremost among them is the thermal stability of phosphoinositide clusters under varying conditions. In this paper we explore the thermal stabilities of PI(4)P, PI(4,5)P₂ and PI(3,4,5)P₃ exposed to either Ca^{2+} or Mg^{2+} . Furthermore, we investigate the stabilizing influence that cholesterol imparts to bivalent cation/PIP clusters.

2. Materials and methods

2.1. Materials

Porcine brain L- α -phosphatidylinositol-4-phosphate (brain PI(4)P) ammonium salt, porcine brain L-α-phosphatidylinositol-4,5-bisphosphate (brain PI(4,5)P₂) ammonium salt, 1,2-dioleoyl-sn-glycero-3phospho-1'-myo-inositol-3,4,5-trisphosphate (DO-PIP₃) ammonium salt, 1.2-dioleovl-sn-glycero-3-phosphocholine (DOPC). plant-derived cholesterol (Chol), and 1-oleoyl-2-[6-[4 (dipyrrometheneborondifluoride)butanovllaminl1-1-hexanovl-sn-glycero-3-phosphoinositol-4. 4,5-bisphosphate, and 3,4,5-triphosphate (TF-PI(4)P, TF-PI(4,5)P₂, TF-PI(3,4,5)P₃) ammonium salts were obtained as powders from Avanti Polar Lipids (Alabaster, Alabama) and used as received. Phosphoinositide lipid stock solutions were prepared by dissolving the powder in a 20:9:1 chloroform:methanol:water mixture by volume while DOPC and cholesterol stocks were dissolved in a 2:1 chloroform:methanol mixture by volume. All lipid stock solutions were stored in concentrations ranging between 1 and 3 mg/mL. Concentrations of the phospholipid stock solutions were determined using a phosphate assay. The purity of lipid stock solutions was monitored on a continuous basis by thin layer chromatography (Rouser, G. 1970). The purity of reagents is reported as listed on the label. Ethylenediaminetetraacetic acid disodium dihydrate (disodium EDTA, 99+% purity) was obtained from Alfa Aesar (Haverhill, MA). Potassium chloride (KCl, 99.999 % trace metal grade), anhydrous magnesium chloride (MgCl₂, 99+% purity), Ethylenediaminetetraacetic acid dipotassium dihydrate (dipotassium EDTA, 99+% purity), sodium hydroxide (NaOH, 99.995 % metal basis), potassium hydroxide (KOH, 99.995 % metal basis), and sodium chloride (NaCl. 99+% purity) were obtained from Thermo Fisher Scientific (Fairlawn, NJ). HEPES free acid (99.5+% pure via titration) and calcium chloride dihydrate (CaCl₂, 99+% purity) were obtained from Sigma Aldrich (St. Louis, MO). HPLC grade chloroform and methanol were also obtained through Fisher Scientific. Deionized water (18.2 M Ω /S) was obtained from a Picopure 3 purification system (Hydro, Durham, NC). For the experiments conducted, potassium-only and sodium-only buffers were prepared.

Buffers

The composition of the sodium-only buffer was 150 mM NaCl, 20 mM HEPES, 1 mM disodium EDTA, pH = 7.4. The composition of the potassium-only buffer was 150 mM KCl, 20 mM HEPES, 1 mM dipotassium EDTA, pH = 7.4. The pH of these buffers was adjusted using 5 M NaOH_(aq) for the sodium-only buffer or 5 M KOH_(aq) for the potassium-only buffer.

2.2. Sample preparation

Lipids, dissolved in volatile organic solvents, were aliquoted from their respective stock solutions into an amber vial to achieve the appropriate mole ratios for the desired vesicle composition. The lipid mixtures were then dried under a steady stream of N_2 gas at 60 $^{\circ}\text{C}$, followed by a 1 hr. drying period in a vacuum oven (15 mmHg). The lipid mixtures were suspended in either the sodium-only or potassium-only buffer which had been warmed to 40 $^{\circ}\text{C}$ beforehand to obtain a suspension of multilamellar vesicles (MLVs). The MLV suspension was

then cycled between a liquid nitrogen bath and a 60 $^{\circ}$ C water bath six times. Following these freeze/thaw cycles, extrusion at room temperature through 100 nm pore filters yielded a stock solution of large unilamellar vesicles (LUVs) with a 1 mM total lipid concentration. LUV sample size and uniformity were measured using a dynamic light scattering instrument (Malvern Panalytical, Malvern, UK) prior to measurements and afterwards to ensure no aggregation occurred as a result of the experimental conditions. Average vesicle diameters were typically narrowly distributed around 120 nm before and after experiments for all conditions.

2.3. Fluorescence measurements

Förster resonance energy transfer (FRET) experiments were carried out using a Perkin Elmer FL 6500 fluorescence spectrophotometer (λ_{ex} / $\lambda_{em} = 490/506$ nm; Ex/Em slit widths = 5/5 nm) equipped with a Peltier thermoelectric heating mantle. LUV samples were diluted using the appropriate buffer from the 1 mM total lipid stock solution to a final concentration of 100 uM and placed into the unit at the desired temperature. Then, the LUVs were allowed to equilibrate for 10 min prior to the first measurement. Step 1: The first measurement was a baseline, with no Ca²⁺ or Mg²⁺ present. Step 2: Prior to the next measurement, Ca²⁺ or Mg²⁺ is added from a concentrated (1 M) stock solution. A 10 min equilibration period transpired before the second set of scans. The new volume was recorded for each measurement. The average of the three scans from each measurement was multiplied by the ratio of the volumes after the addition to the initial volume to account for the effect of dilution on fluorescence intensity. To consider the temperature dependence of fluorescence intensities, we normalized the fluorescence intensities at each temperature to the fluorescence intensity measured in the absence of bivalent cations (Step 1). We propagated the error using the standard deviations between scans, which is significantly smaller than the deviation between experiments. This means that all initial measurements are normalized to 1 +/- the standard deviation between scans, while the second measurements represent a deviation from the initial condition without bivalent cations present. The resulting error present in each graph is thus the error from multiple repeat experiments.

2.4. Data analysis

To determine statistical significance in each data set a one-way ANOVA (95 % confidence interval) analysis was performed, followed by a Šídák multiple comparisons test. This test compares the initial condition means to the experimental condition means and generates a p-value as a measure of statistical significance between the two data sets. For each condition an N-value and p-value are given. The N value represents the number of repeat experiments, and the p-value is a measure of statistical difference. In each graph that displays a significant difference, stars are present which represent the level of statistical difference. **** = $p \leq 0.0001$, *** = $p \leq 0.001$, ** = $p \leq 0.05$. Analyses are conducted using GraphPad Prism© software (San Diego, CA).

3. Results and discussion

3.1. Thermal stability of bivalent cation/PIP clusters

The aim of this study is twofold: first, to ascertain the degree of formation and thermal stability of PI(4)P, PI(4,5)P₂ and PI(3,4,5)P₃ domains in the presence of Mg²⁺ or Ca²⁺; secondly to investigate whether the formation of bivalent cation/PIP domains is affected by the presence of cholesterol. Our study is structured as follows to address these inquiries:

(a) To characterize PIP domain stability, we conducted fluorescence quenching experiments at 20°C and 80°C, respectively. We chose

this temperature range strategically: if PIP/bivalent cation domains are present in model systems at temperatures as high as 80°C, they are also likely to exist at physiological temperatures in the more complex environments of native membranes. Conversely, if these domains are not observed at 20°C for specific PIP/bivalent cation systems, they also are not likely to exist at physiological temperatures in biological membranes. In the cases where the domains melt between 20°C and 80°C, in principle, follow up experiments could determine the domain melting temperature (as it turns out this is not possible due to width of the melting transition and a comparably small fluorescence intensity change). For monitoring PIP domain formation, we employed TopFlour labeled PIPs (mixed in with unlabeled PIPs) which undergo Homo-FRET (quenching) when in proximity due to domain formation.

- (b) The interaction of bivalent cations with PIPs depends on the overall charge of the lipid which is a function of the number of phosphomonoester groups at the inositol ring. To compare the stability of PIP/bivalent cation domains for PIPs with different number of phosphomonoester groups at the inositol ring, we investigate this aspect for PI(4)P, PI(4,5)P₂ and PI(3,4,5)P₃.
- (c) We had previously found that even in the absence of bivalent cations PIPs exhibit mild and very fragile clustering when Na⁺ was present, while K⁺ does not stabilize PIP clusters (Han et al., 2020; Han et al., 2022; Redfern and Gericke, 2005). Therefore, we investigate the effect of Mg²⁺ and Ca²⁺ cations on PIP domain formation in the presence of Na⁺ or K⁺.
- (d) To explore the effect of cholesterol on bivalent cation/PIP domain formation, we compare the results obtained in the absence with those obtained in the presence of cholesterol.
- (e) In our experiments, Ca²⁺ or Mg²⁺ is added to preformed vesicles, allowing us to monitor increases in domain formation. Fluorescence intensities are strongly temperature dependent. Therefore, we normalize the data relative to the fluorescence intensities observed prior to the addition of the bivalent cations at 20°C and 80°C, respectively. This allows us to compare the effect of bivalent cation addition at 20°C and 80°C. Although we can infer information about domains existing before the addition of the bivalent cation from these experiments, we do not directly measure pre-existing domains.

Fig. 2 shows fluorescence quenching for the interaction of PI(4)P in ${\rm K^+}$ or ${\rm Na^+}$ -based buffers upon the addition of ${\rm Mg^{2+}}$ or ${\rm Ca^{2+}}$. The binding of ${\rm Mg^{2+}}$ to PIPs is significantly weaker than the corresponding binding of ${\rm Ca^{2+}}$ (Wen et al., 2018, 2021) and hence we are using a higher concentration for Mg²⁺ (10 mM) than for Ca²⁺ (5 mM). We deliberately employ concentrations exceeding physiological levels to ensure a robust response in case PIP clustering occurs (Mg^{2+} :PIP mole ratio 10000:1 and Ca²⁺/PIP mole ratio 5000:1). The panels A and B in Fig. 2 show the fluorescence change upon the addition of Mg²⁺ and Ca²⁺ at 20°C and 80°C for a K⁺-based buffer, while panel C and D show the corresponding data for a Na⁺-based buffer. In general, it is expected that PI(4)P shows prior to the addition of the respective bivalent cation no clustering in a K⁺ based buffer and minimal clustering in a Na⁺ based buffer (Redfern and Gericke, 2004). At 20°C, the addition of Mg²⁺ or Ca²⁺ does not significantly alter the fluorescence intensity, regardless of the buffer system. At 80°C, a minimal decrease in fluorescence intensity is noted, albeit at the threshold of statistical significance. This experimental approach is designed to monitor enhanced clustering upon the addition of the respective bivalent cation. In Fig. 2, the data demonstrate that at 20° C, the interaction between PI(4)P and Mg $^{2+}$ or Ca $^{2+}$ in a Na $^+$ -based buffer does not lead to a notable increase in cluster formation. However, at 80°C a slight increase in clustering is observed, albeit minimally. This indicates that at 20°C, there is some limited clustering in the absence of bivalent cations, as it was also observed previously for saturated acyl chain PI(4)P (Redfern and Gericke, 2004). These clusters appear to melt

Fig. 1. : Chemical structures of PI(4)P, PI(4,5)P₂ and PI(3,4,5)P₃. At physiological pH and ionic strength, the charges are about -2 (PI(4)P), -4 (PI(4,5)P₂ and -5 (PI (3,4,5)P₃). While we are using the same mole fractions of PIPs in the lipid mixtures, the charge of the vesicles will differ due to the different charges of the PIPs.

somewhere between 20° C and 80° C, as evidenced by the minor decrease in fluorescence upon the addition of the respective bivalent cation at 80° C. The comparison of the fluorescence intensity drop at 20° C and 80° C in a K⁺-based buffer reveals a slight decrease fluorescence intensity (statistically not significant) upon the addition of bivalent cations at both temperatures, indicating that at neither temperature, PI(4)P enriched domains exist in the absence of bivalent cations. Overall, the clustering effect of bivalent cations on PI(4)P is marginal.

Fig. 3 illustrates the degree of fluorescence quenching observed for PI(4,5)P $_2$ in K $^+$ or Na $^+$ based buffers following the addition of Mg $^{2+}$ or Ca $^{2+}$. For both buffer systems, the fluorescence intensity change upon the addition of Mg $^{2+}$ to PC/PI(4,5)P $_2$ vesicles at 20°C is marginal. At 80°C, a statistically significant decrease of the fluorescence is observed for the Na $^+$ based buffer (indicating enhanced domain formation), while for the K $^+$ based buffer the decrease is in the same range as the decrease at 20°C, however, for both temperatures the intensity drop is at the limit of statistical relevance. In contrast to Mg $^{2+}$, significant decreases in fluorescence intensity were noted when Ca $^{2+}$ was added, regardless of the buffer conditions and temperature. At 20 °C, the average fluorescence decreases relative to the initial condition by about 20 % for both the K $^+$ - and Na $^+$ based buffer. At 80 °C, the addition of Ca $^{2+}$ results in an average fluorescence intensity decrease of 35–40 %. The smaller fluorescence intensity decrease at 20°C compared to 80°C is due to the pre-existing domains in particular in the Na $^+$ -based buffer.

In Fig. 4, the extent of fluorescence quenching upon the addition of Ca^{2+} or Mg^{2+} to $\text{PI}(3,4,5)\text{P}_3/\text{PC}$ vesicles is depicted. Similar to what was observed for $\text{PI}(4,5)\text{P}_2$, the addition of Mg^{2+} to mixed $\text{PC}/\text{PI}(3,4,5)\text{P}_3$ vesicles results in only a slight reduction in fluorescence intensity. Specifically, in a K⁺ based buffer, the fluorescence intensity decreases by 2–3 % on average at 20°C and 4–5 % at 80°C. For the Na⁺ based buffer, the fluorescence intensity remains essentially unchanged. However, upon adding Ca^{2+} , we observe a statistically significant drop in fluorescence intensities for both buffer systems (6–8 %) at 20°C and 80°C. The fluorescence intensity drop for $\text{PI}(3,4,5)\text{P}_3$ upon the addition of Ca^{2+} is less pronounced than what was observed for $\text{PI}(4,5)\text{P}_2$, indicating a less robust domain formation. Like for the other investigated PIPs, the impact of Mg^{2+} on $\text{PI}(3,4,5)\text{P}_3$ clustering is marginal.

3.2. Impact of cholesterol on the thermal stability of bivalent cation/PIP domains

It has been previously established that cholesterol stabilizes phosphoinositide enriched domains (Jiang et al., 2014; Wen et al., 2018). Furthermore, coarse grained MD simulations have shown that cholesterol prefers interacting with anionic lipids over neutral lipids

(Yesylevskyy and Demchenko, 2012), which should promote PIP/cholesterol domain formation. To investigate the effect of cholesterol on the formation and thermal stability of bivalent cation/PIP clusters, we repeated the experiments from the previous section with 40 mol% cholesterol present in the lipid mixture (the concentration of the PIP species was kept constant, while the DOPC concentration is reduced to 58 %).

Prior research from our lab has shown that the presence of cholesterol promotes PI(4)P clustering (Jiang et al., 2014). Fig. 5 displays the change in fluorescence intensity upon the addition of $\mathrm{Mg^{2+}}$ or $\mathrm{Ca^{2+}}$ for a mixture that contains in addition to DOPC (58 mol%), PI(4)P (1.84 mol%) and TF-PI(4)P (0.16 mol%) also 40 mol% cholesterol. The addition of $\mathrm{Mg^{2+}}$ does not result in a decrease of fluorescence intensity irrespective of the buffer composition (Na⁺ and K⁺ based buffer) and temperature, indicating that the extent of PI(4)P clustering is unchanged. In the presence of $\mathrm{Ca^{2+}}$ the drop in fluorescence intensity is slightly more pronounced, but also in this case the change in fluorescence intensity is not statistically significant. Overall, the data suggest that while cholesterol promotes PI(4)P clustering (Jiang et al., 2014), the extent of PI(4)P/cholesterol domain formation is not enhanced by the presence of $\mathrm{Ca^{2+}}$ and $\mathrm{Mg^{2+}}$.

The effect of bivalent cations on PI(4,5)P2/cholesterol clusters is shown in Fig. 6. The effect of Mg²⁺ in a K⁺ based buffer is marginal at both investigated temperatures. In a Na⁺ based buffer, we observe only a small reduction of fluorescence intensity at 20°C, however, at 80°C the drop in intensity is statistically significant. This suggests that the PI(4,5) P₂/cholesterol domains that exist at 20°C in the absence of Mg²⁺ (see Graber et al. (2012)) disintegrate somewhere between 20°C and 80°C. The addition of Mg²⁺ stabilizes the PI(4,5)P₂/cholesterol up to a temperature of 80°C. This is consistent with the data presented in Fig. 3, where we saw no fluorescence intensity changes in a K⁺ based buffer and only a marginal increase of Mg²⁺ induced clustering in a Na⁺ based buffer at 20°C and statistically significant increase of clustering at 80°C. At 20°C, the addition of Ca²⁺ results in a significant decrease of fluorescence intensity in both buffer systems like what was observed in the absence of cholesterol. When comparing the effect of Ca^{2+} on $PI(4,5)P_2$ clustering in the absence and presence of cholesterol, we find for the K⁺ based buffer a similar drop in fluorescence intensity for the two lipid mixtures (~20 %). In contrast, for the Na⁺ based buffer, the fluorescence intensity drop in the presence of cholesterol is less pronounced than in its absence. This suggests that PI(4,5)P₂/cholesterol domains are less developed in the absence of Ca²⁺ in a K⁺ based buffer compared to a Na⁺ based buffer. Consequently, the increase in clustering (decrease in fluorescence intensity) upon addition of Ca²⁺ is more pronounced in a K⁺ based buffer. At 80°C, the decrease in fluorescence intensity

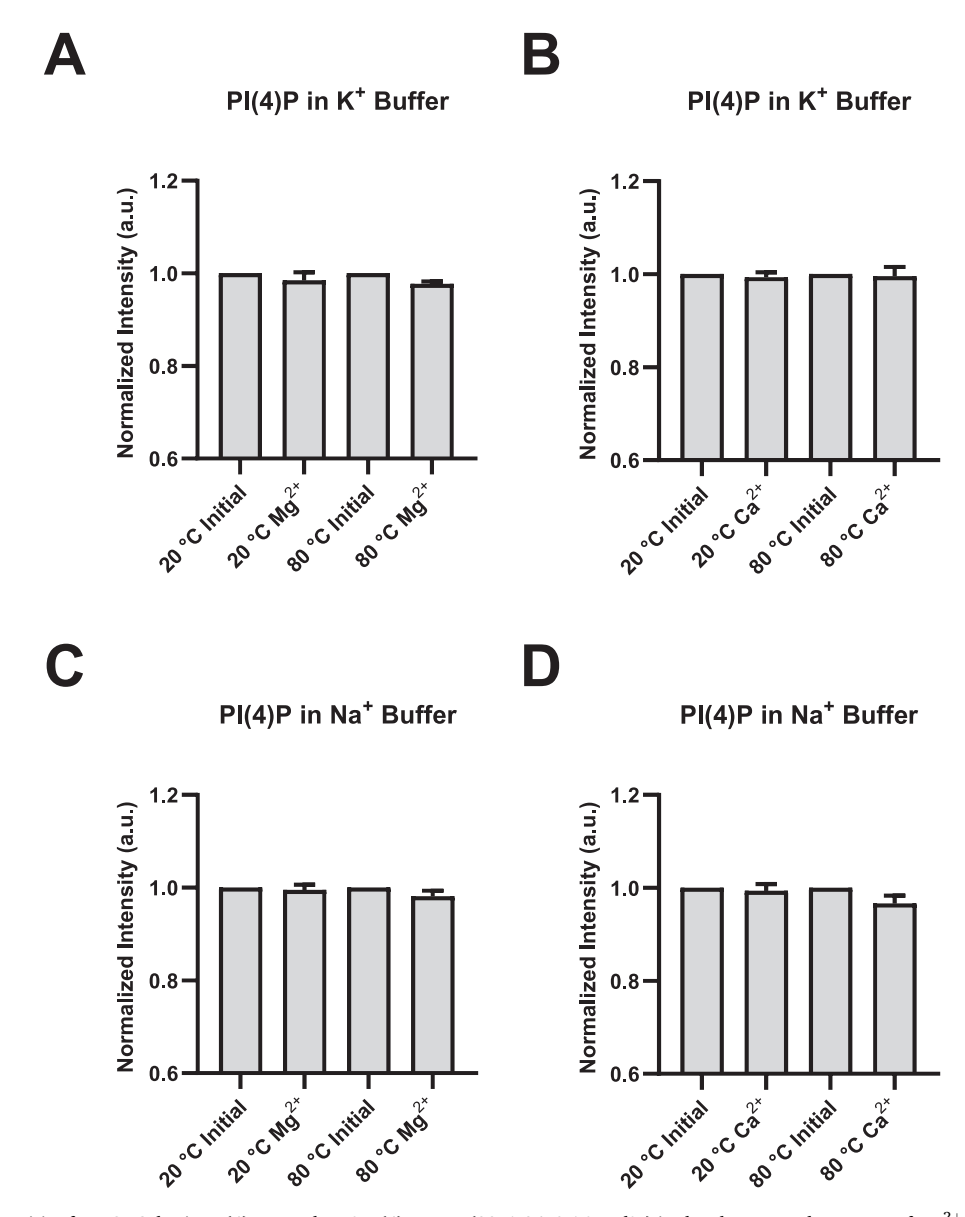


Fig. 2. Fluorescence intensities for DOPC/brain-PI(4)P/TopFluor®PI(4)P LUVs (98/1.84/0.16 mol%) in the absence and presence of Mg^{2+} or Ca^{2+} prepared in either sodium or potassium based buffer. The normalized intensities at each temperature are calculated by setting the fluorescence intensity in the absence of bivalent cations as the reference value (1.0) and reporting the intensities in the presence of bivalent cations relative to this reference. Panel A and B: Effect of the addition of Mg^{2+} or Ca^{2+} on PI(4)P clustering in a K^+ based buffer. Panel C and D: Effect of the addition of Mg^{2+} or Ca^{2+} on PI(4)P clustering in a K^+ based buffer. For all investigated conditions, little to no decrease of fluorescence intensity was observed, indicating that neither Mg^{2+} nor Ca^{2+} cluster PI(4)P appreciably. Bivalent cation free buffer: 150 mM NaCl or KCl, 1 mM Na_2 EDTA or K_2 EDTA, 20 mM HEPES, pH 7.4. After the addition of the bivalent cation stock solution, the final sample concentration is 5 mM Ca^{2+} or 10 mM Ca^{2+

(increase in the extent of $PI(4,5)P_2$ clustering) is for both buffer systems similar in the absence and presence of cholesterol (see Fig. 3 for comparison). This suggests that the $PI(4,5)P_2$ /cholesterol domains have disintegrated at $80^{\circ}C$ and the observed decline is due to the formation of $PI(4,5)P_2/Ca^{2+}$ clusters. Based upon our data it cannot be unequivocally delineated whether cholesterol is or is not present in these domains. However, since cholesterol and Ca^{2+} synergistically stabilize at $20^{\circ}C$ PI $(4,5)P_2$ enriched domains, this is also likely the case at $80^{\circ}C$.

The impact of bivalent cations on PI(3,4,5)P₃/cholesterol clusters is depicted in Fig. 7. As observed for PI(4,5)P₂, the impact of Mg^{2+} on PI (3,4,5)P₃/cholesterol is marginal, with a slightly stronger but statistically not significant decrease for the Na⁺ based buffer at 80°C. Upon the addition of Ca²⁺, a fluorescence intensity drop is observed for all investigated buffer conditions and temperatures. The extent of the decrease in fluorescence intensity (increase in clustering), is similar to

the extent of clustering increase in the absence of cholesterol. Previous studies from our lab have demonstrated that cholesterol promotes PI $(3,4,5)P_3$ domain formation at room temperature (Jiang et al., 2014). The addition of Ca^{2+} results in additional clustering, however, the effect is significantly less pronounced than what was observed for the PI(4,5) P_2 /cholesterol system. The consistent decrease in fluorescence intensity upon the addition of Ca^{2+} at both temperatures is intriguing. In general, this observation could be attributed to the absence of cholesterol/PI(3,4,5) P_3 domains at $20^{\circ}C$ or, alternatively, the persistence of these domains at $80^{\circ}C$. The comparison of the experiments when Ca^{2+} is added in the absence of cholesterol (Fig. 4, B/D) with the corresponding experiments in its presence (Fig. 7, B/D), reveals similar fluorescence intensity drops in both cases. This suggests that cholesterol/PI(3,4,5) P_3 domains for the experimental conditions used in our current experiments do not exist or are not developed well enough so that fluorescence quenching occurs. In

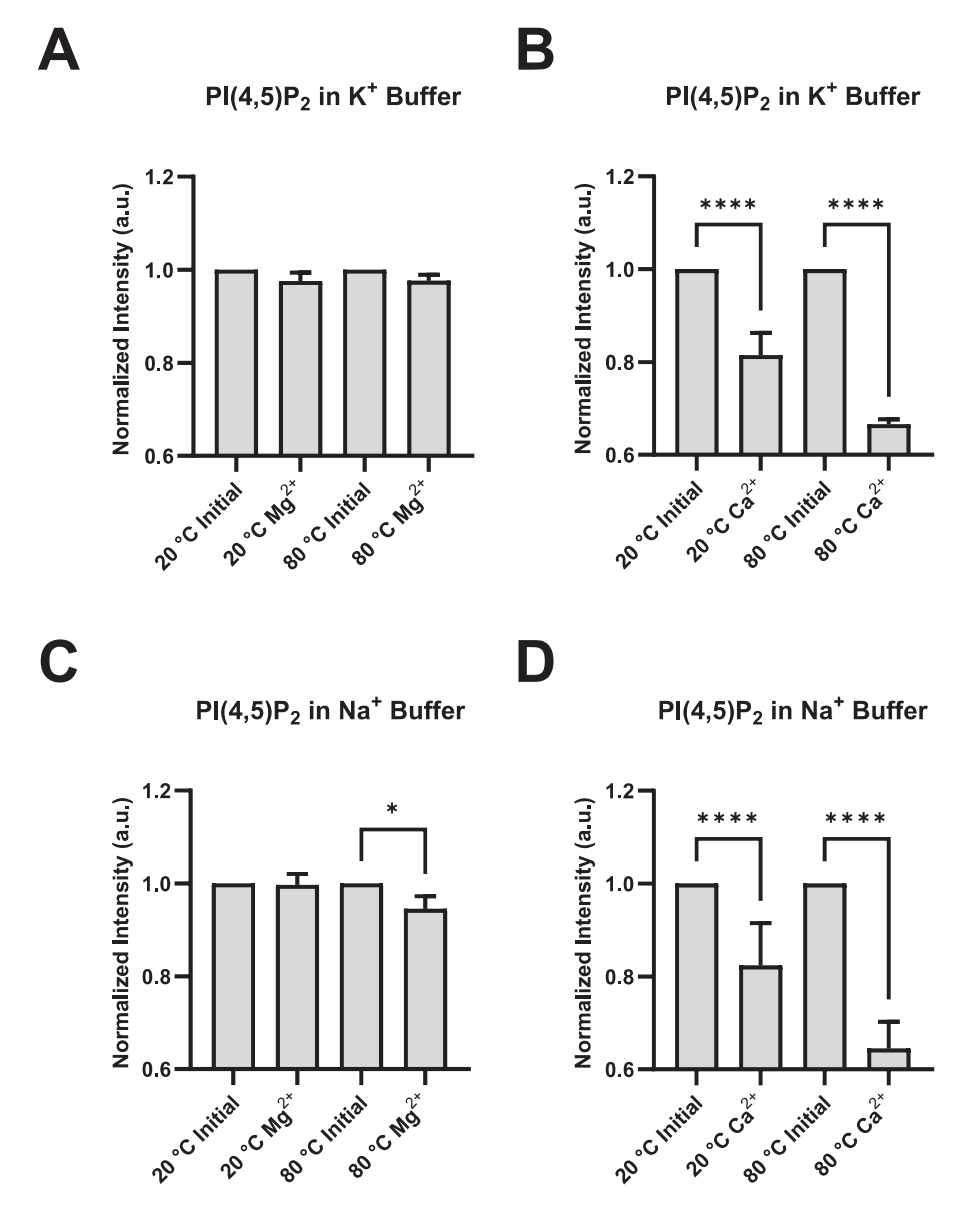


Fig. 3. Fluorescence intensities for DOPC/brain-PI(4,5)P₂/TopFluor®PI(4,5)P₂ LUVs (98/1.84/0.16 mol%) in the absence and presence of Mg^{2+} or Ca^{2+} prepared in either sodium or potassium based buffer. The normalized intensities at each temperature are calculated by setting the fluorescence intensity in the absence of bivalent cations as the reference value (1.0) and reporting the intensities in the presence of bivalent cations relative to this reference. Panel A and B: Effect of the addition of Mg^{2+} or Ca^{2+} on PI(4,5)P₂ clustering in a K^+ based buffer. Panel C and D: Effect of the addition of Mg^{2+} or Ca^{2+} on PI(4,5)P₂ clustering in a Na^+ based buffer. For the addition of Mg^{2+} , only at 80°C and a Na^+ based buffer a statistically significant drop in fluorescence intensity is observed. In contrast, for the addition of Ca^{2+} a decrease in fluorescence is observed for all conditions. Bivalent cation free buffer: 150 mM NaCl or KCl, 1 mM Na_2 EDTA or K_2 EDTA, 20 mM HEPES, pH 7.4. After the addition of the bivalent cation stock solution, the final sample concentration is 5 mM Ca^{2+} or 10 mM Mg^{2+} , respectively. The total lipid concentration is 100 μ M. All reported data are the averages of five completely independent experiments; error bars represent standard deviations. The single * represents $p \leq 0.005$, while **** represents $p \leq 0.0001$.

contrast, for giant unilamellar vesicles composed of 20 mol% PI(3,4,5) $P_3/80$ mol% palmitoyloleoylphosphatidylcholine (POPC) we did observe domain formation (Jiang et al., 2014). We attribute the difference between our earlier and current experiments to the significantly different lipid compositions (POPC vs. DOPC and 20 mol% vs. 2 mol% PI (3,4,5) P_3).

4. Conclusions

Previous studies using MD simulation (Han et al., 2020; Han et al., 2022; Slochower et al., 2015) and wet lab experiments (Wen et al., 2018, 2021) have demonstrated that the interaction between ${\rm Mg}^{2+}$ ions and PI (4,5)P₂ is weak. In contrast, the interaction with Ca²⁺ ions results in significant clustering of PI(4,5)P₂. In this work, we extend these

investigations to include other phosphoinositides, specifically PI(4)P and PI(3,4,5)P₃. Our findings indicate that the interaction of Mg^{2+} with various phosphoinositides is weak across all investigated species, as evidenced by only a marginal increase in clustering. The interaction of Ca^{2+} with PI(4)P leads to only a very limited increase of clustering, which is a clear departure from what is observed for the higher phosphorylated PIP species. It is remarkable that the interaction of Ca^{2+} with PI(3,4,5)P₃ leads to a significantly smaller drop in fluorescence intensity than what is observed for the PI(4,5)P₂/ Ca^{2+} interaction, despite its larger charge. This finding suggests that the clustering effect of Ca^{2+} on PI(3,4,5)P₃ is less than the corresponding clustering for PI(4,5)P₂.

The $Ca^{2+}/PI(4,5)P_2$ and $Ca^{2+}/PI(3,4,5)P_3$ clusters show a remarkable thermal stability. The fact that these domains exist at these high temperatures underscores the strong binding of Ca^{2+} to $PI(4,5)P_2$ and PI

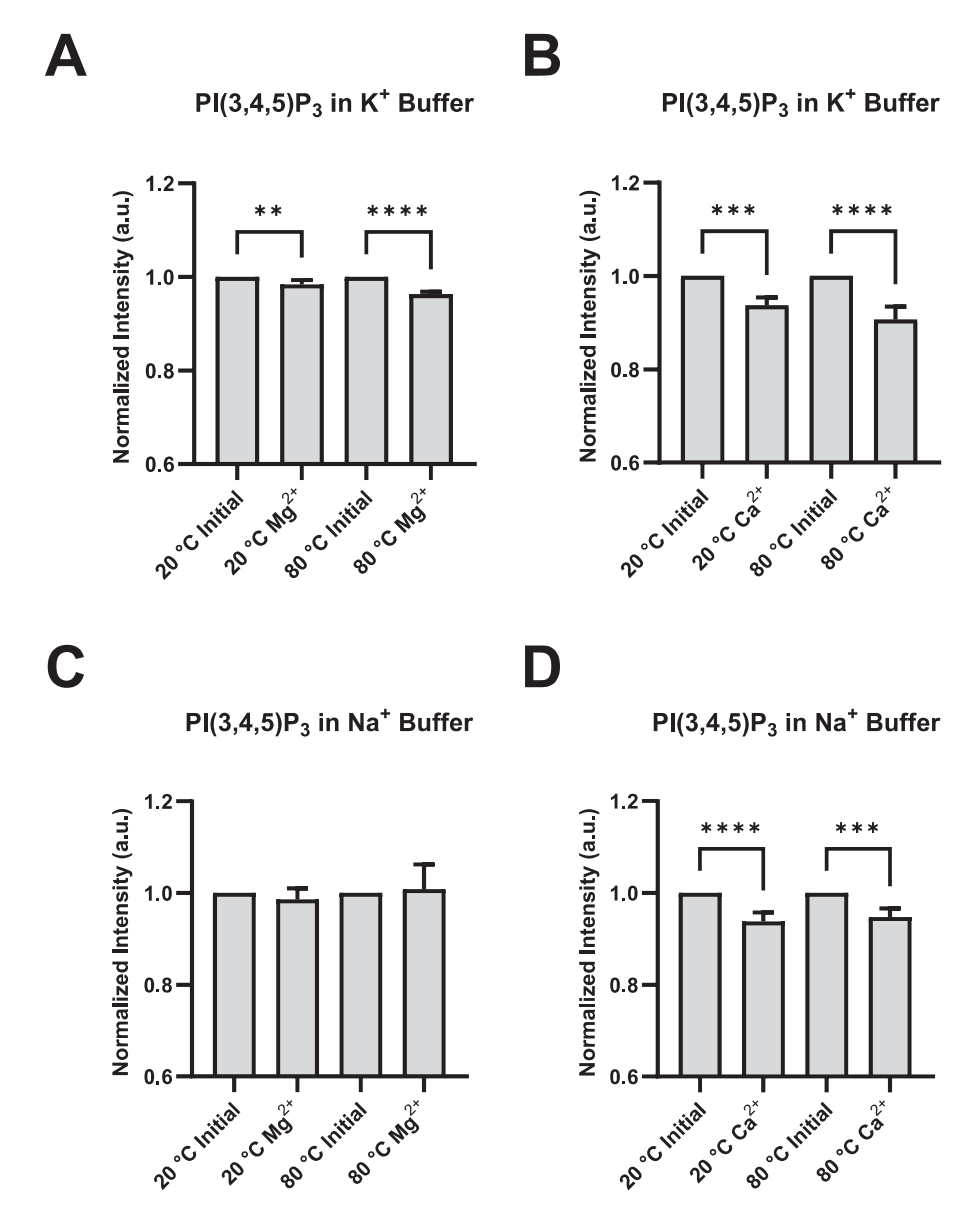


Fig. 4. Fluorescence intensities for DOPC/brain-PI(3,4,5)P₃/TopFluor®PI(3,4,5)P₃ LUVs (98/1.84/0.16 mol%) in the absence and presence of Mg^{2+} or Ca^{2+} prepared in either sodium or potassium based buffer. The normalized intensities at each temperature are calculated by setting the fluorescence intensity in the absence of bivalent cations as the reference value (1.0) and reporting the intensities in the presence of bivalent cations relative to this reference. Panel A and B: Effect of the addition of Mg^{2+} or Ca^{2+} on PI(3,4,5)P₃ clustering in a K^+ based buffer. Panel C and D: Effect of the addition of Mg^{2+} or Ca^{2+} on PI(3,4,5)P₃ clustering in a Na^+ based buffer. For the addition of Mg^{2+} , only no or marginal changes of the fluorescence intensity are observed. For the addition of Ca^{2+} statistically significant changes are observed for both buffers at $20^{\circ}C$ and $80^{\circ}C$. Bivalent cation free buffer: 150 mM NaCl or KCl, 1 mM Na_2 EDTA or K_2 EDTA, 20 mM HEPES, pH 7.4. After the addition of the bivalent cation stock solution, the final sample concentration is 5 mM Ca^{2+} or 10 mM Ca^{2+} , respectively. The total lipid concentration is 100μ M. All reported data are the averages of five completely independent experiments; error bars represent standard deviations. The ** represents $p \leq 0.001$ and **** represents $p \leq 0.0001$.

 $(3,4,5)P_3$, respectively. This suggests that such clusters also exist at physiological temperatures in more complex environments like it is found in biological membranes. While in this study Mg^{2+} and Ca^{2+} concentrations were used that exceed cellular levels, studies from the Feigenson group (Wen et al., 2018) showed that $Ca^{2+}/PI(4,5)P_2$ clusters are also formed at physiological Ca^{2+} concentrations.

The effect of bivalent cations on PIP/cholesterol domains depends on the nature of the phosphoinositide. The weak interaction between bivalent cations and PI(4)P observed in absence of cholesterol persists even in lipid mixtures containing both cholesterol and phospholipids. Although the fluorescence intensity decreases slightly more in the presence of cholesterol, it is statistically not significant. The lack of Ca²⁺/PI(4)P clustering is surprising considering that phosphatidic acid, which also carries a singular phosphomonoester group, shows strong

clustering in the presence of Ca²⁺ (Faraudo and Travesset, 2007; Kouaouci et al., 1985; Laroche et al., 1991). While PI(4)P probably forms dimers in the presence of Ca²⁺, we believe that larger clusters cannot form due to steric reasons. Clustering would require that the PI (4)P headgroup positions itself in a way that more than two lipids can be bridged. An arrangement where the inositol rings are side by side (like it is probably happening for PI(4,5)P2) would result in a phosphomonoester/phosphomonoester distance that is too large to be bridged by the Ca²⁺. A "face-to-face" packing of the inositol ring would move the phosphomonoester groups of adjacent molecules closer together (principally allowing for effective Ca²⁺ bridging), however, the axial OH group in the 2-position of the inositol ring might prevent such a packing. In the future, it might be of interest to compare the results obtained for PI(4)P corresponding data to the for the other

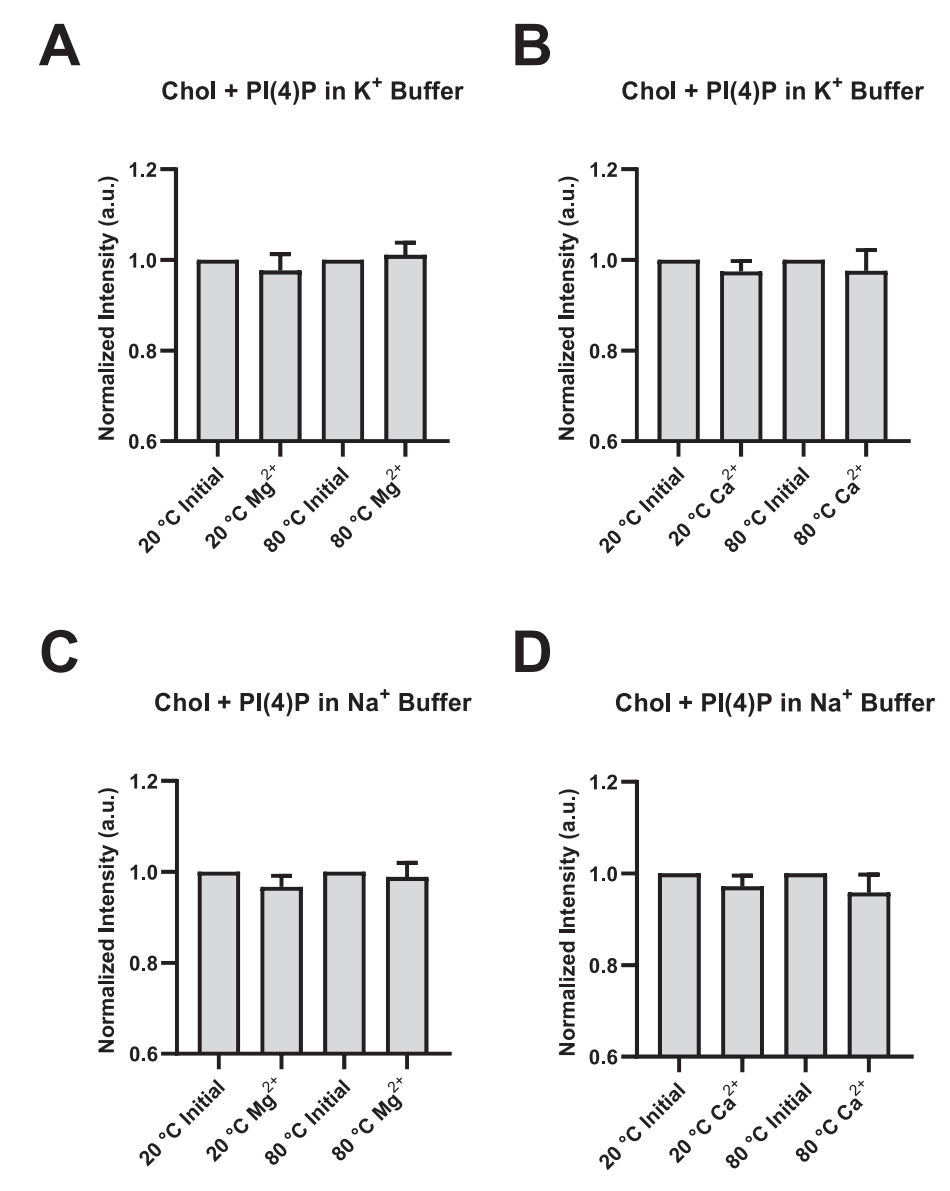


Fig. 5. Fluorescence intensities for Cholesterol/DOPC/brain-PI(4)P/TopFluor®PI(4)P LUVs (40/58/1.84/0.16 mol%) in the absence and presence of Mg^{2+} or Ca^{2+} prepared in either sodium or potassium based buffer. The normalized intensities at each temperature are calculated by setting the fluorescence intensity in the absence of bivalent cations as the reference value (1.0) and reporting the intensities in the presence of bivalent cations relative to this reference. Panel A and B: Effect of the addition of Mg^{2+} or Ca^{2+} on PI(4)P clustering in a K^+ based buffer. Panel C and D: Effect of the addition of Mg^{2+} or Ca^{2+} on PI(4)P clustering in a Na^+ based buffer. For both, the addition of Mg^{2+} and Ca^{2+} , only marginal changes of the fluorescence intensity are observed. Bivalent cation free buffer: 150 mM NaCl or KCl, 1 mM Na_2 EDTA or K_2 EDTA, 20 mM HEPES, pH 7.4. After the addition of the bivalent cation stock solution, the final sample concentration is 5 mM Ca^{2+} or 10 mM Ca^{2+} , respectively. The total lipid concentration is 100 μ M. All reported data are the averages of six completely independent experiments; error bars represent standard deviations.

phosphatidylinositolmonophosphates, PI(3)P and PI(5)P.

Cholesterol and Ca^{2+} synergistically stabilize $PI(4,5)P_2$ enriched domains. At $20^{\circ}C$, the fluorescence intensity drop upon the addition of Ca^{2+} in the presence of cholesterol is less pronounced than in its absence, highlighting the existence of $PI(4,5)P_2$ /cholesterol domains prior to the addition of Ca^{2+} and the additional domain stabilizing effect of Ca^{2+} . However, at $80^{\circ}C$, $PI(4,5)P_2$ /cholesterol domains have dissolved and hence the fluorescence drop upon the addition of Ca^{2+} is in the same range as in the absence of cholesterol. The interaction of $PI(4,5)P_2$ with Mg^{2+} is also in the presence of cholesterol marginal. Overall, the geometry of $PI(4,5)P_2$ seems to be more favorable for clustering compared to PI(4)P and $PI(3,4,5)P_3$.

For the $PI(3,4,5)P_3$ containing lipid system, it seems that the extent of domain formation in the presence of cholesterol is limited and the domain formation upon the addition of Ca^{2+} (or Mg^{2+}) is similar to the

cholesterol free case. The fact that $PI(3,4,5)P_3$ shows in comparison to $PI(4,5)P_2$ reduced Ca^{2+} induced clustering, raises the question whether Ca^{2+} promotes for the other 3-phosphorylated PIP species clustering. An MD simulation showed no $PI(3,5)P_2$ clustering in the presence of Ca^{2+} (Bradley et al., 2020), however, $PI(3,5)P_2$ is different from $PI(4,5)P_2$ since it has isolated rather than neighbored phosphomonoester groups. In this context, it would be interesting to investigate the clustering of phosphatidylinositol-3,4-bisphosphate.

A range of important cellular processes have been associated with PIP clustering. It is important to note that clustering of PI(4)P upon the addition of Ca^{2+} or Mg^{2+} does not occur. If PI(4)P clustering is observed in a cellular context, other interaction partners (other lipid or proteins) must have contributed to such clustering. $\text{Ca}^{2+}/\text{PI}(4,5)P_2$ clusters show a remarkable thermal stability. Wen et al. (2018) showed for room temperature experiments that Ca^{2+} clusters PI(4,5)P₂ at physiological

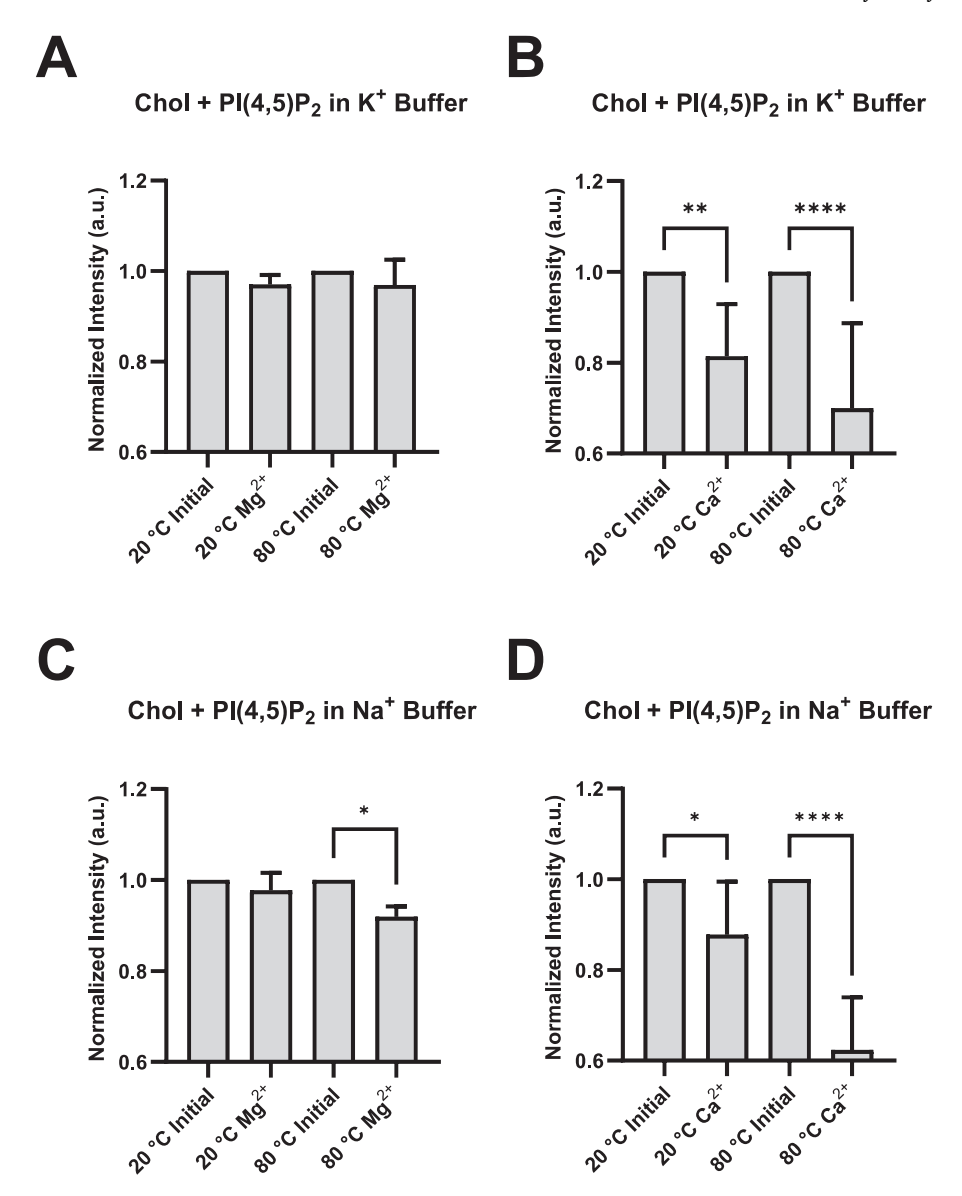


Fig. 6. Fluorescence intensities for Chol/DOPC/brain-PI(4,5)P₂/TopFluor®PI(4,5)P₂ LUVs (40/58/1.84/0.16 mol%) in the absence and presence of Mg^{2+} or Ca^{2+} prepared in either sodium or potassium based buffer. The normalized intensities at each temperature are calculated by setting the fluorescence intensity in the absence of bivalent cations as the reference value (1.0) and reporting the intensities in the presence of bivalent cations relative to this reference. Panel A and B: Effect of the addition of Mg^{2+} or Ca^{2+} on PI(4,5)P₂ clustering in a K^+ based buffer. Panel C and D: Effect of the addition of Mg^{2+} or Ca^{2+} on PI(4,5)P₂ clustering in a K^+ based buffer a statistically significant change in fluorescence intensity is observed. The addition of Kg^{2+} or all investigated temperatures and buffer systems. Bivalent cation free buffer: 150 mM NaCl or KCl, 1 mM Na₂EDTA or K_2 EDTA, 20 mM HEPES, pH 7.4. After the addition of the bivalent cation stock solution, the final sample concentration is 5 mM K_2 - or 10 mM K_2 -, respectively. The total lipid concentration is 100 μM. All reported data are the averages of six completely independent experiments; error bars represent standard deviations. The single * represents K_2 - or K_3 - or K_4 - or K

concentrations (Ca^{2+} concentration $\sim 6~\mu M$). Taken together these results reaffirm that $Ca^{2+}/PI(4,5)P_2$ clusters exist under physiological temperatures and lipid/cation concentrations.

Notably, PI(3,4,5)P $_3$ accumulation is associated with various physiological processes, particularly in chemotactic migration of eukaryotic cells. In this context, PI(4,5)P $_2$ /PI(3,4,5) $_3$ gradients play a crucial role in proper cell movement (Devreotes and Horwitz, 2015). Ca $^{2+}$ and PI(3,4,5)P $_3$ drive the targeting of signaling proteins from the cytoplasm to the leading edge of the migrating cell (Falke and Ziemba, 2014). The observation that Ca $^{2+}$ /PI(3,4,5)P $_3$ /Ca $^{2+}$ clusters appear to be less dense than the PI(4,5)P $_2$ /Ca $^{2+}$ clusters might have implications for the dynamic behavior of these clusters at the leading edge.

CRediT authorship contribution statement

Greta E. Schmidt: Investigation, Data curation. **Alonzo H. Ross:** Writing – original draft, Supervision, Funding acquisition, Conceptualization. **Trevor A. Paratore:** Writing – original draft, Investigation, Formal analysis, Data curation, Conceptualization. **Arne Gericke:** Writing – original draft, Supervision, Project administration, Methodology, Funding acquisition, Conceptualization.

Declaration of Generative AI and AI-assisted technologies in the writing process

During the preparation of this work the authors used Copilot in order to improve the language and readability. After using this tool, the

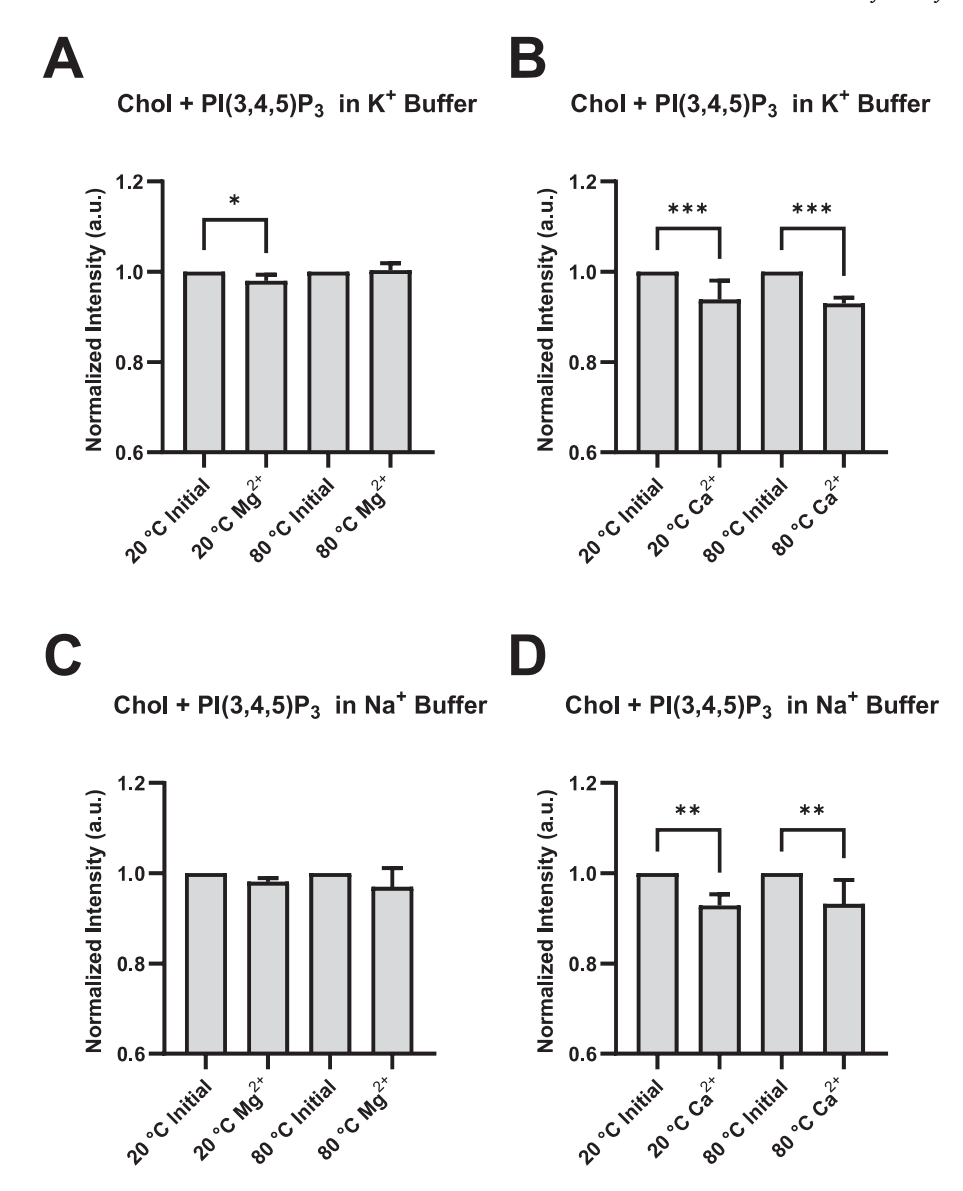


Fig. 7. Fluorescence intensities for Chol/DOPC/brain-PI(3,4,5)P₃/TopFluor®PI(3,4,5)P₃ LUVs (40/58/1.84/0.16 mol%) in the absence and presence of Mg^{2+} or Ca^{2+} prepared in either sodium or potassium based buffer. The normalized intensities at each temperature are calculated by setting the fluorescence intensity in the absence of bivalent cations as the reference value (1.0) and reporting the intensities in the presence of bivalent cations relative to this reference. Panel A and B: Effect of the addition of Mg^{2+} or Ca^{2+} on PI(3,4,5)P₃ clustering in a K^+ based buffer. Panel C and D: Effect of the addition of Mg^{2+} or Ca^{2+} on PI(3,4,5)P₃ clustering in a K^+ based buffer. For the addition of Mg^{2+} , only no or marginal changes of the fluorescence intensity are observed. For the addition of Ca^{2+} statistically significant changes are observed for both buffers at $20^{\circ}C$ and $80^{\circ}C$. Bivalent cation free buffer: 150 mM NaCl or KCl, 1 mM Na_2 EDTA or K_2 EDTA, 20 mM HEPES, pH 7.4. After the addition of the bivalent cation stock solution, the final sample concentration is 5 mM Ca^{2+} or 10 mM Mg^{2+} , respectively. The total lipid concentration is $100 \mu M$. All reported data are the averages of five completely independent experiments; error bars represent standard deviations. The * represents $p \leq 0.05$, the ** represents $p \leq 0.01$.

authors reviewed and edited the content as needed and take full responsibility for the content of the publication.

Data Availability

Data will be made available on request.

Acknowledgements

This work was supported by NSF CHE 1904886 and NSF CHE 1950512.

References

Bradley, R.P., Slochower, D.R., Janmey, P.A., Radhakrishnan, R., 2020. Divalent cations bind to phosphoinositides to induce ion and isomer specific propensities for nanocluster initiation in bilayer membranes. R. Soc. Open Sci. 7, 192208.

Bucki, R., Wang, Y.H., Yang, C., Kandy, S.K., Fatunmbi, O., Bradley, R., Pogoda, K., Svitkina, T., Radhakrishnan, R., Janmey, P.A., 2019. Lateral distribution of phosphatidylinositol 4,5-bisphosphate in membranes regulates formin- and ARP2/3-mediated actin nucleation. J. Biol. Chem. 294, 4704–4722.

Bura, A., Cabrijan, S., Duric, I., Bruketa, T., Jurak Begonja, A., 2023. A plethora of functions condensed into tiny phospholipids: the story of PI4P and PI(4,5)P(2). Cells

Cabral-Dias, R., Antonescu, C.N., 2022. Control of phosphatidylinositol-3-kinase signaling by nanoscale membrane compartmentalization. Bioessays, e2200196.
Catimel, B., Schieber, C., Condron, M., Patsiouras, H., Connolly, L., Catimel, J., Nice, E. C., Burgess, A.W., Holmes, A.B., 2008. The PI(3,5)P2 and PI(4,5)P2 interactomes.
J. Proteome Res. 7, 5295–5313.

- Catimel, B., Yin, M.-X., Schieber, C., Condron, M., Patsiouras, H., Catimel, J., Robinson, D.E.J.E., Wong, L.S.-M., Nice, E.C., Holmes, A.B., Burgess, A.W., 2009. PI(3,4,5)P3 Interactome. J. Proteome Res. 8, 3712-3726.
- Collins, K.D., 1997. Charge density-dependent strength of hydration and biological structure. Biophys. J. 72, 65–76.
- Conduit, S.E., Davies, E.M., Fulcher, A.J., Oorschot, V., Mitchell, C.A., 2021. Superresolution microscopy reveals distinct phosphoinositide subdomains within the cilia transition zone. Front Cell Dev. Biol. 9, 634649.
- Devreotes, P., Horwitz, A.R., 2015. Signaling networks that regulate cell migration. Cold Spring Harb. Perspect. Biol. 7, a005959.
- Drucker, P., Pejic, M., Galla, H.J., Gerke, V., 2013. Lipid segregation and membrane budding induced by the peripheral membrane binding protein annexin A2. J. Biol. Chem. 288, 24764–24776.
- Epand, R.M., Vuong, P., Yip, C.M., Maekawa, S., Epand, R.F., 2004. Cholesterol-dependent partitioning of Ptdlns(4,5)P-2 into membrane domains by the N-terminal fragment of NAP-22 (neuronal axonal myristoylated membrane protein of 22 kDa). Biochem. J. 379, 527–532.
- Falke, J.J., Ziemba, B.P., 2014. Interplay between phosphoinositide lipids and calcium signals at the leading edge of chemotaxing ameboid cells. Chem. Phys. Lipids 182, 73–79
- Faraudo, J., Travesset, A., 2007. Phosphatidic acid domains in membranes: effect of divalent counterions. Biophys. J. 92, 2806–2818.
- Fratini, M., Krishnamoorthy, P., Stenzel, I., Riechmann, M., Matzner, M., Bacia, K., Heilmann, M., Heilmann, I., 2021. Plasma membrane nano-organization specifies phosphoinositide effects on Rho-GTPases and actin dynamics in tobacco pollen tubes. Plant Cell 33, 642–670.
- Gambhir, A., Hangyas-Mihalye, G., Zaitseva, I., Cafiso, D.S., Wang, J., Murray, D., Pentyala, S.N., Smith, S.O., McLaughlin, S., 2004. Electrostatic sequestration of PIP2 on phospholipid membranes by basic/aromatic regions of proteins. Biophys. J. 86, 2188–2207.
- Graber, Z.T., Gericke, A., Kooijman, E.E., 2014. Phosphatidylinositol-4,5-bisphosphate ionization in the presence of cholesterol, calcium or magnesium ions. Chem. Phys. Lipids 182, 62–72.
- Graber, Z.T., Jiang, Z., Gericke, A., Kooijman, E.E., 2012. Phosphatidylinositol-4,5-bisphosphate ionization and domain formation in the presence of lipids with hydrogen bond donor capabilities. Chem. Phys. Lipids 165, 696–704.
- Gregory, K.P., Elliott, G.R., Robertson, H., Kumar, A., Wanless, E.J., Webber, G.B., Craig, V.S.J., Andersson, G.G., Page, A.J., 2022. Understanding specific ion effects and the Hofmeister series. Phys. Chem. Chem. Phys. 24, 12682–12718.
- Han, K., Gericke, A., Pastor, R.W., 2020. Characterization of specific ion effects on PI (4,5)P2 clustering: molecular dynamics simulations and graph-theoretic analysis. J. Phys. Chem. B 124, 1183–1196.
- Han, K., Kim, S.H., Venable, R.M., Pastor, R.W., 2022. Design principles of PI(4,5)P2 clustering under protein-free conditions: specific cation effects and calcium-potassium synergy. Proc. Natl. Acad. Sci. U. S. A. 119, e2202647119.
- He, X., Ewing, A.G., 2023. Hofmeister series: from aqueous solution of biomolecules to single cells and nanovesicles. Chembiochem 24, e202200694.
- Jiang, Z., Redfern, R.E., Isler, Y., Ross, A.H., Gericke, A., 2014. Cholesterol stabilizes fluid phosphoinositide domains. Chem. Phys. Lipids 182, 52–61.
- Katan, M., Cockcroft, S., 2020. Phosphatidylinositol(4,5)bisphosphate: diverse functions at the plasma membrane. Essays Biochem 64, 513–531.
- Kooijman, E.E., King, K.E., Gangoda, M., Gericke, A., 2009. Ionization properties of phosphatidylinositol polyphosphates in mixed model membranes. Biochemistry 48, 9360–9371
- Kouaouci, R., Silvius, J.R., Graham, I., Pezolet, M., 1985. Calcium-induced lateral phase separations in phosphatidylcholine-phosphatidic acid mixtures. A Raman spectroscopic study. Biochemistry 24, 7132–7140.
- Laroche, G., Dufourc, E.J., Dufourcq, J., Pezolet, M., 1991. Structure and dynamics of dimyristoylphosphatidic acid/calcium complexes by 2H NMR, infrared, spectroscopies and small-angle x-ray diffraction. Biochemistry 30, 3105–3114.
- Levental, I., Byfield, F.J., Chowdhury, P., Gai, F., Baumgart, T., Janmey, P.A., 2009a. Cholesterol-dependent phase separation in cell-derived giant plasma-membrane vesicles. Biochem. J. 424, 163–167.
- Levental, I., Cebers, A., Janmey, P.A., 2008. Combined electrostatics and hydrogen bonding determine intermolecular interactions between polyphosphoinositides. J. Am. Chem. Soc. 130, 9025–9030.
- Levental, I., Christian, D.A., Wang, Y.-H., Madara, J.J., Discher, D.E., Janmey, P.A., 2009b. Calcium-dependent lateral organization in phosphatidylinositol 4,5bisphosphate (PIP2)- and cholesterol-containing monolayers. Biochemistry 48, 8241–8248.

- Li, D., Sun, F., Yang, Y., Tu, H., Cai, H., 2022. Gradients of PI(4,5)P2 and PI(3,5)P2 jointly participate in shaping the back state of dictyostelium cells. Front Cell Dev. Biol. 10, 835185.
- Li, X., Miao, Y., Pal, D.S., Devreotes, P.N., 2020. Excitable networks controlling cell migration during development and disease. Semin. Cell Dev. Biol. 100, 133–142.
- Lolicato, F., Saleppico, R., Griffo, A., Meyer, A., Scollo, F., Pokrandt, B., Muller, H.M., Ewers, H., Hahl, H., Fleury, J.B., Seemann, R., Hof, M., Brugger, B., Jacobs, K., Vattulainen, I., Nickel, W., 2022. Cholesterol promotes clustering of PI(4,5)P2 driving unconventional secretion of FGF2. J. Cell Biol. 221.
- Mandal, K., 2020. Review of PIP2 in cellular signaling, functions and diseases. Int. J. Mol. Sci. 21.
- Musse, A.A., Gao, W., Homchaudhuri, L., Boggs, J.M., Harauz, G., 2008. Myelin basic protein as a "PI(4,5)P2-modulin": a new biological function for a major central nervous system protein. Biochemistry 47, 10372–10382.
- Myeong, J., Park, C.G., Suh, B.C., Hille, B., 2021. Compartmentalization of phosphatidylinositol 4,5-bisphosphate metabolism into plasma membrane liquidordered/raft domains. Proc. Natl. Acad. Sci. U.S.A. 118.
- Overduin, M., Kervin, T.A., 2021. The phosphoinositide code is read by a plethora of protein domains. Expert Rev. Proteom. 18, 483–502.
- Owusu Kwarteng, D., Putta, P., Kooijman, E.E., 2021. Ionization properties of monophosphoinositides in mixed model membranes. Biochim Biophys. Acta Biomembr. 1863, 183692.
- Palmieri, M., Nowell, C.J., Condron, M., Gardiner, J., Holmes, A.B., Desai, J., Burgess, A. W., Catimel, B., 2010. Analysis of cellular phosphatidylinositol (3,4,5)-trisphosphate levels and distribution using confocal fluorescent microscopy. Anal. Biochem. 406, 41–50
- Redfern, D.A., Gericke, A., 2004. Domain formation in phosphatidylinositol monophosphate/ phosphatidylcholine model membrane systems. Biophys. J. 86, 2980–2992.
- Redfern, D.A., Gericke, A., 2005. pH dependent microdomain formation in phosphatidylinositol polyphosphate/ phosphatidylcholine mixed vesicles. J. Lip Res 46, 504–515.
- Redpath, G.M.I., Betzler, V.M., Rossatti, P., Rossy, J., 2020. Membrane heterogeneity controls cellular endocytic trafficking. Front Cell Dev. Biol. 8, 757.
- Rouser, G., Fkeischer, S., Yamamoto, A., 1970. Two dimensional thin layer chromatographic separation of polar lipids and determination of phospholipids by phosphorus analysis of spots. Lipids 5, 494–496.
- Sarmento, M.J., Borges-Araujo, L., Pinto, S.N., Bernardes, N., Ricardo, J.C., Coutinho, A., Prieto, M., Fernandes, F., 2021. Quantitative FRET microscopy reveals a crucial role of cytoskeleton in promoting PI(4,5)P2 confinement. Int. J. Mol. Sci. 22.
- Siess, K.M., Leonard, T.A., 2019. Lipid-dependent Aktivity: where, when, and how. Biochem. Soc. Trans. 47, 897–908.
- Slochower, D.R., Huwe, P.J., Radhakrishnan, R., Janmey, P.A., 2013. Quantum and allatom molecular dynamics simulations of protonation and divalent ion binding to phosphatidylinositol 4,5-bisphosphate (PIP2). J. Phys. Chem. B 117, 8322–8329.
- Slochower, D.R., Wang, Y.H., Radhakrishnan, R., Janmey, P.A., 2015. Physical chemistry and membrane properties of two phosphatidylinositol bisphosphate isomers. Phys. Chem. Chem. Phys.
- Tong, J., Nguyen, L., Vidal, A., Simon, S.A., Skene, J.H., McIntosh, T.J., 2008. Role of GAP-43 in sequestering phosphatidylinositol 4,5-bisphosphate to Raft bilayers. Biophys. J. 94, 125–133.
- Viaud, J., Mansour, R., Antkowiak, A., Mujalli, A., Valet, C., Chicanne, G., Xuereb, J.M., Terrisse, A.D., Severin, S., Gratacap, M.P., Gaits-Iacovoni, F., Payrastre, B., 2016. Phosphoinositides: important lipids in the coordination of cell dynamics. Biochimie 125, 250–258.
- Wang, J., Gambhir, A., Hangyas-Mihalyne, G., Murray, D., Golebiewska, U., McLaughlin, S., 2002. Lateral sequestration of phosphatidylinositol 4,5-bisphosphate by the basic effector domain of myristoylated alanine-rich C kinase substrate is due to nonspecific electrostatic interactions. J. Biol. Chem. 277, 34401–34412.
- Wang, Y.H., Slochower, D.R., Janmey, P.A., 2014. Counterion-mediated cluster formation by polyphosphoinositides. Chem. Phys. Lipids 182, 38–51.
- Wen, Y., Vogt, V.M., Feigenson, G.W., 2018. Multivalent cation-bridged PI(4,5)P2 clusters form at very low concentrations. Biophys. J. 114, 2630–2639.
- Wen, Y., Vogt, V.M., Feigenson, G.W., 2021. PI(4,5)P2 clustering and its impact on biological functions. Annu. Rev. Biochem.
- Yesylevskyy, S.O., Demchenko, A.P., 2012. How cholesterol is distributed between monolayers in asymmetric lipid membranes. Eur. Biophys. J. 41, 1043–1054.
- Yoshioka, D., Fukushima, S., Koteishi, H., Okuno, D., Ide, T., Matsuoka, S., Ueda, M., 2020. Single-molecule imaging of PI(4,5)P2 and PTEN in vitro reveals a positive feedback mechanism for PTEN membrane binding. Commun. Biol. 3, 92.